DOI: 10.1002/chem.201000180

AT-Specific DNA Binding of Binuclear Ruthenium Complexes at the Border of Threading Intercalation

Johanna Andersson,[a] Minna Li,[b] and Per Lincoln*[a]

Abstract: The binuclear ruthenium complex $[\mu\text{-bidppz(phen)}_4\text{Ru}_2]^{4+}$ has been extensively studied since the discovery of its unusual threading intercalation interaction with DNA, a binding mode with extremely slow binding and dissociation kinetics. The complex has been shown to be selective towards long stretches of alternating AT base pairs, which makes it interesting, for example, as a model compound for anti-malaria drugs due to the high AT content of the genome of the malaria parasite *P. falciparum*. We have investigated the effect of bridging ligand structure on threading intercalation ability and found that length and rigidity as well as the size of the intercalated ring system are all factors that affect the rate and selectivity of the threading intercalation. In particular, we discovered a new DNA-threading compound, $[\mu\text{-dppzip(phen)}_4\text{Ru}_2]^{4+}$, which appears to be just at the border of being capable of threading intercalation and displays even greater selectivity for AT-DNA than the parent compound, $[\mu\text{-bidppz(phen)}_4\text{Ru}_2]^{4+}$.

Keywords: DNA · enantioselectivity · intercalations · ruthenium · sequence selectivity

Introduction

Since Barton et al.'s pioneering studies of the DNA-binding properties of Δ- and Λ-$[\text{Ru(phen)}_3]^{2+}$ 26 years ago, ruthenium complexes and their interactions with DNA have been intensively studied for their potential use as DNA probes, photoreagents and inhibitors of DNA-related cellular processes.[1–3] However, the majority of these studies have concerned mononuclear complexes and only recently have binuclear ruthenium complexes, which in general show greater selectivity due to increased size and higher binding affinity due to increased charge, started to receive attention.[4–7] Of these, the semi-rigid binuclear ruthenium complex $[\mu\text{-bidppz(phen)}_4\text{Ru}_2]^{4+}$ (phen = 1,10-phenanthroline and bidppz = 11,11′-bi(dipyrido[3,2-*a*:2′,3′-*c*]phenazinyl)), complex **1** in Scheme 1, is of particular interest in the context of potential biological activity because it has been shown to bind DNA by threading intercalation, an unusual binding

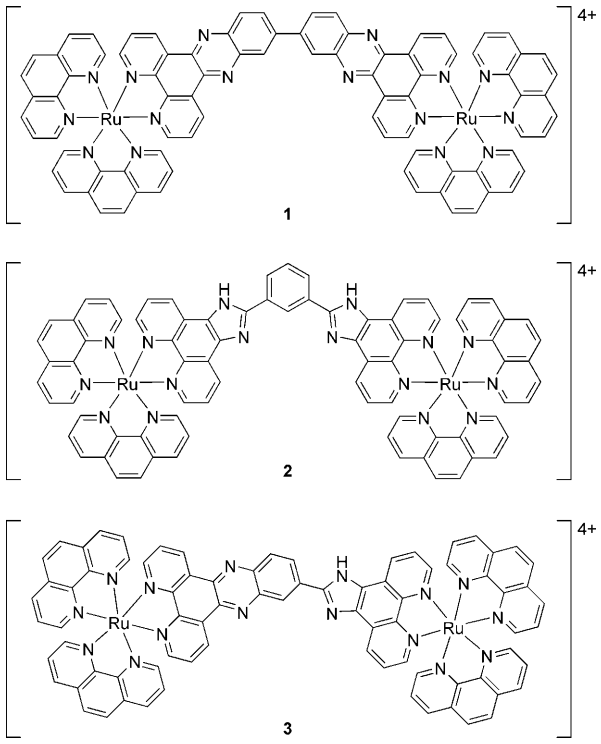

Scheme 1. Structure of the ruthenium complexes $[\mu\text{-bidppz(phen)}_4\text{Ru}_2]^{4+}$ (**1**), $[\mu\text{-bipb(phen)}_4\text{Ru}_2]^{4+}$ (**2**) and $[\mu\text{-dppzip(phen)}_4\text{Ru}_2]^{4+}$ (**3**).

[a] J. Andersson, Prof. P. Lincoln
Department of Chemical and Biological Engineering
Chalmers University of Technology, 41296 Gothenburg (Sweden)
Fax: (+46) 31-772-3858
E-mail: lincoln@chalmers.se

[b] Dr. M. Li
College of Pharmaceutical Sciences, Capital Medical University
No 10 Xitoutiao, You An Men, Beijing 100069 (P. R. China)

Supporting information for this article is available on the WWW under http://dx.doi.org/10.1002/chem.201000180.

mode in which the bridging ligand is intercalated between base pairs with the two ruthenium centres positioned in opposite grooves (see Figure 1). To reach this threaded state,

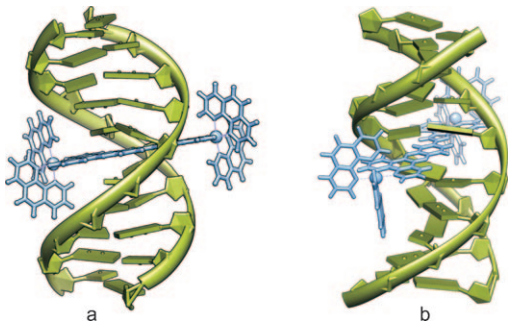

Figure 1. Threading intercalation of ΛΛ-**3** in DNA: a) side-view and b) view from the major groove.

and also to dissociate from it, the ruthenium complex has to pass one of its bulky coordinated ruthenium centres through the base-pair stack, which occurs with extremely slow kinetics.[8] The latter, in particular, is an important feature for the inhibition of DNA-related biological processes such as transcription,[9] and compounds with low dissociation rates, such as nogalamycin, are known to show high cytotoxicity.[10,11] The threading intercalation of **1** has been shown to be kinetically selective towards long tracts of alternating AT base pairs,[12] a property that could potentially be used to target AT-rich sequences frequently found at functionally important locations in the genome such as promoter regions and origins of replications[13,14] and in some unicellular parasites, for example, the malaria parasite *P. falciparum*.[15]

The majority of binuclear ruthenium complexes reported in the literature are designed to preferentially bind the DNA grooves and therefore have bridging ligands that are either too short[4,16–22] or lack extended aromatic ring systems[7,23,24] for threading intercalation to be likely to occur. There are, however, a few binuclear complexes with structures similar to **1** that theoretically could thread DNA, but to the best of our knowledge no such observations have so far been reported.[6,25] With the exception of **1**, the only binuclear ruthenium complex known to bind DNA by threading intercalation is the closely related rigid analogue [μ-dtpf-(phen)$_4$Ru$_2$]$^{4+}$ (dtpf = 4,5,9,12,16,17,21,25-octaaza-23*H*-ditriphenyleno[2,3-*b*:2′,3′-*h*]fluorene), which shows slightly slower threading kinetics and higher dissociation rates than **1**.[26,27] Note also that the flexibly linked dppz dimer [μ-c4-(cpdppz)$_2$(phen)$_4$Ru$_2$]$^{4+}$ (c4(cpdppz)$_2$ = *N*,*N*′-bis(12-cyano-12,13-dihydro-11*H*-cyclopenta[*b*]dipyrido[3,2-*h*:2′,3′-*j*]phenazine-12-carbonyl)-1,4-diaminobutane) threads the linker through the DNA, which results in a bis-intercalation binding mode in which both ruthenium centres end up in the same groove.[28]

Chao et al. have previously reported the synthesis and DNA-binding studies of racemic [μ-bipb(phen)$_4$Ru$_2$]$^{4+}$ (bipb = 1,3-bis(imidazo[4,5-*f*][1,10]phenanthrolin-2-yl)benzene),[5] complex **2** in Scheme 1, which is of a similar overall size to **1** but has a bridging ligand that is expected to be more flexible due to the two pivotal single bonds. It has been reported to interact with calf thymus DNA by intercalation of the bridging ligand. However, the compound has never been assayed for threading intercalation and therefore in this work we have studied its interactions with both calf thymus DNA (ct-DNA) and poly(dAdT)$_2$ (AT-DNA) more thoroughly. To further investigate the effect of the bridging ligand on the threading intercalation, which hopefully will be of value for the future design of new threading intercalating compounds, we also synthesised and studied the hybrid complex [μ-dppzip(phen)$_4$Ru$_2$]$^{4+}$ (dppzip = 2-(dipyrido[3,2-*a*:2′,3′-*c*]phenazin-11-yl)imidazo[4,5-*f*][1,10]phenanthroline), complex **3** in Scheme 1, which has a substantially shorter bridging ligand than **1** but retains the rigidity and the extended aromatic ring system of the parent compound. Because the threading intercalation kinetics of complex **1** have been found to be sensitive to the chirality of ruthenium coordination[12] and dialysis experiments with racemic complex **2** have revealed enantioselective binding,[5] the pure enantiomers of complexes **2** and **3** were synthesised and studied in this work.

Results

Synthesis: The pure enantiomers of the new complexes **2** and **3** were synthesised from enantiopure bis(1,10-phenanthroline)(1,10-phenanthroline-5,6-dione)ruthenium bis(hexafluorophosphate) (compound **a** in Scheme 2) prepared according to the procedure previously described by Hiort et al.[29] Pure enantiomers of complex **2** were successfully obtained by treating isophthalaldehyde (**b**) with 2 equiv of **a** in the presence of ammonium acetate under slightly acidic con-

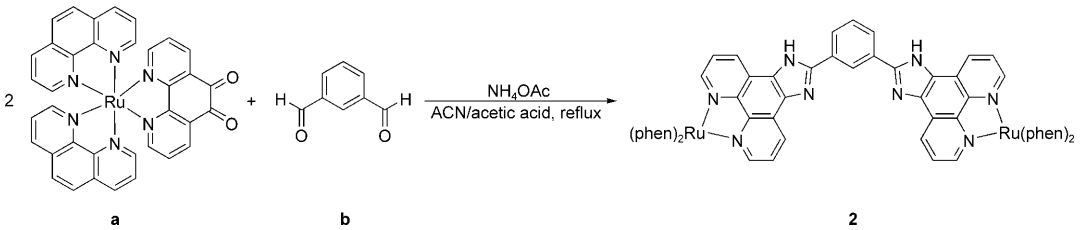

a b 2

Scheme 2. Synthesis of complex **2**.

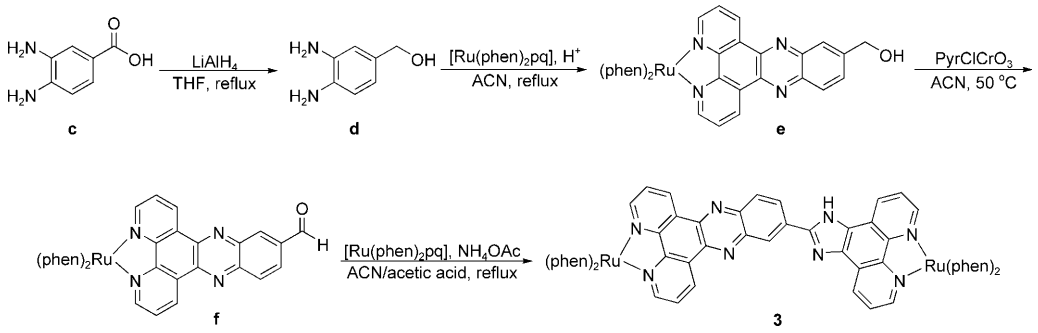

Scheme 3. Synthesis of complex **3**.

ditions (Scheme 2). The product was obtained as the chloride salt, which gave a different ^{1}H NMR spectrum (see the Experimental section) to that previously reported by Chao et al. for the racemic [μ-bipb(phen)$_4$Ru$_2$](ClO$_4$)$_4$.[5] However, addition of increasing amounts NaClO$_4$ to the NMR sample caused the two peaks at $\delta = 9.54$ and 9.15 ppm to move upfield and finally end up very close to each other resembling a doublet. Other peaks were also affected by the addition of NaClO$_4$ and eventually the spectrum appeared very similar to that previously reported.

The synthesis of complex **3** is shown in Scheme 3. 1,2-Diamino-4-hydroxymethylbenzene (**d**) was prepared from 3,4-diaminobenzoic acid (**c**) by reduction with LiAlH$_4$ and then treated with **a** under slightly acidic conditions to produce the hydroxymethyl-substituted Ru-dppz complex **e**, as previously described by Li and Lincoln.[30] The hydroxymethyl group was oxidised by pyridinium chlorochromate at 50 °C to form the aldehyde **f**. The rate of this reaction seems to be very sensitive to the experimental conditions and the reaction is better monitored by TLC to ensure the formation of the aldehyde and avoid over-oxidation to the carboxylic acid. The reaction was stopped as soon as the carboxylic acid, which has a much lower R_f value than the alcohol and aldehyde, appeared on the TLC plates. The aldehyde was then treated with **a** in the presence of ammonium acetate, following the same procedure as that used to produce complex **2**, to form the imidazole ring of complex **3**. Although the chloride salt of complex **2** was easily obtained by precipitation with tetrabutylammonium chloride in acetone, a large excess of the ammonium salt had to be added to a very concentrated solution of complex **3** to obtain the chloride salt in good yield.

Absorption spectroscopy: The absorption spectra of the three ruthenium complexes in 150 mM NaCl solution are shown in Figure 2. All three complexes exhibit absorption bands of similar shapes at around 260 nm, which indicates that the bridging ligand does not have any significant effect on the $\pi \rightarrow \pi^*$ transitions of the phenanthroline ligands. The differences in the absorption spectra of the three complexes above 300 nm can be attributed mainly to differences between the $\pi \rightarrow \pi^*$ transitions of the bridging ligands.

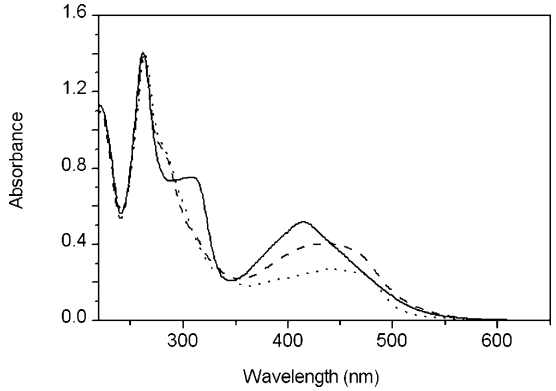

Figure 2. Absorption spectra of ΔΔ-**1** (solid), ΔΔ-**2** (dotted) and ΔΔ-**3** (dashed) in 150 mM NaCl solution.

All three complexes exhibit hypochromism in the absorption bands between 350 and 550 nm in the presence of DNA, although the effect on **2** was less pronounced than on the other two complexes (see the Supporting Information). In addition, a small redshift of these absorption bands was observed for all complexes, which seemed to be slightly larger in the presence of ct-DNA than with AT-DNA. ΔΔ-**2**, but not ΛΛ-**2**, in the presence of ct-DNA displayed an overall decrease in absorbance probably due to condensation of the DNA and the complex (see below).

Circular dichroism: The high enantiomeric purity of the newly synthesised complexes was confirmed by circular dichroism (CD). As shown in Figure 3, the CD spectra of the enantiomers of both **2** and **3** are quite similar to the spectra of the corresponding enantiomers of **1**. However, note that the signal at 268 nm decreases significantly on going from the bidppz-bridged complex **1** to the bipb-bridged complex **2**. On the other hand, **2** shows a substantially larger signal at 300 nm than the other two complexes, which indicates that the total rotary strength is more or less conserved in the band system between 250 and 350 nm. This suggests that the decrease in the signal at 268 nm is due to differences in the coupling of the electronic transitions rather than in the coordination geometry or enantiomeric purity.

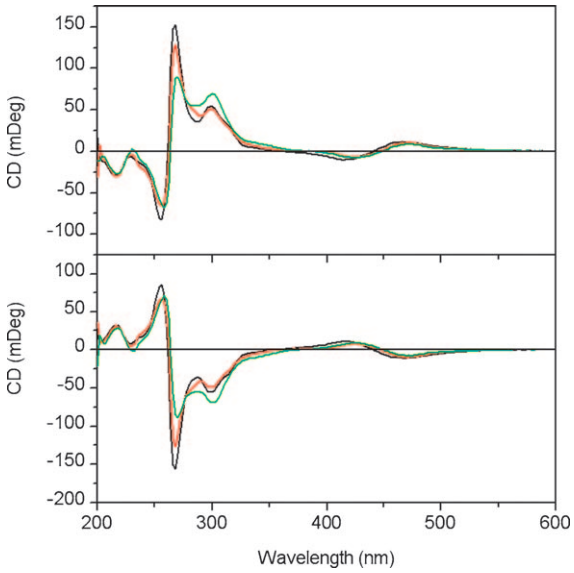

Figure 3. Circular dichroism spectra of the ΛΛ (top) and ΔΔ enantiomers (bottom) of complexes **1** (black), **2** (green) and **3** (red) at a concentration of 7 μM in 150 mM NaCl solution.

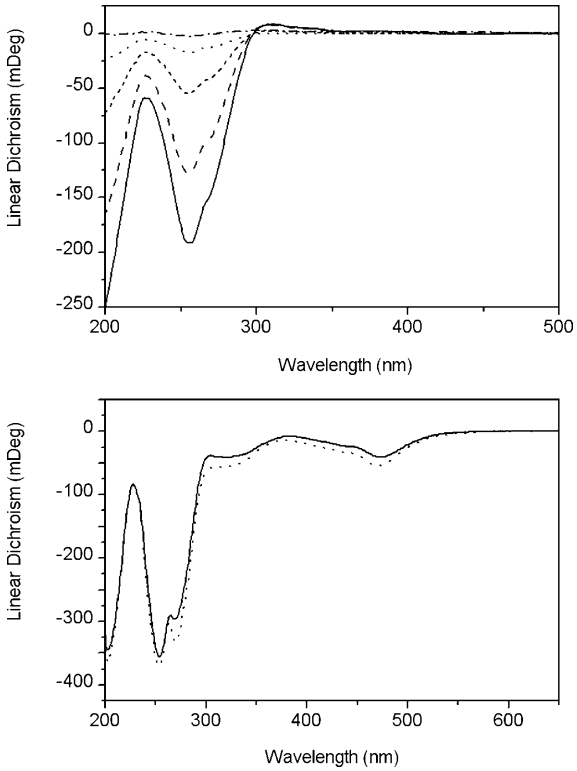

Figure 4. Top: Linear dichroism spectra of ΔΔ-**2** in the presence of ct-DNA at different complex/base-pair ratios (——=1:18, – – –=1:16, -----=1:12, •••••=1:11, –•–•–=1:10). The DNA signal disappears, which indicates complete condensation, at a complex/base-pair ratio of around 1:10. Bottom: Linear dichroism spectra of ΔΔ- (solid) and ΛΛ-**3** (dotted) in the presence of ct-DNA.

Linear dichroism: Linear dichroism (LD) measurements revealed that **2** interacts with ct-DNA in an unexpected manner: both enantiomers seem to reversibly condense the DNA with the ΔΔ enantiomer being more effective in doing so. Titration of the complex into DNA samples of constant concentration resulted in complete condensation, that is, no LD signal from DNA, at the complex/base-pair ratio of around 1:10 for the ΔΔ enantiomer (see Figure 4, top), whereas for the ΛΛ enantiomer the DNA signal was reduced by nearly a factor five for the same complex/base-pair ratio. For the ΛΛ enantiomer, a weak negative signal at around 475 nm and a small but significant positive phenanthroline peak at 265 nm were observed. Importantly, upon addition of sodium dodecyl sulfate (SDS), the initial intensity of the DNA signal was immediately recovered for both enantiomers.

The LD spectra of both enantiomers of **3** with ct-DNA are strikingly similar (see Figure 4, bottom) compared with the pronounced diastereomeric differences shown by the LD spectra of the enantiomers of **1** before and after threading intercalation. The LD spectra of **3** show significant negative peaks at around 320 and 475 nm, a less prominent negative peak at around 420 nm and a positive peak (on the negative background of the nucleobase band) at 265 nm, characteristic of the phenanthroline ligands. The shape of the spectra remained unchanged after heating for 16 h at 50 °C, however, the intensities of the peaks decreased slightly. After addition of SDS to the samples, none of the complex peaks could be detected by LD, which indicates fast dissociation of the complex. These results should be contrasted with those of the known threading intercalator **1**, which for the ΔΔ enantiomer shows substantial spectral changes when heated in the presence of ct-DNA, going from positive to negative peaks between 300 and 550 nm, and resistance to SDS sequestration after heating.

Unfortunately, LD measurements could not be performed on AT-DNA samples because the currently commercially available poly(dAdT)$_2$ was too short to obtain sufficient orientation in the flow cell.

Luminescence: The steady-state emission spectra of the new complexes were examined in both water and acetonitrile purged with nitrogen. Complex **2** exhibits luminescence in aqueous solution with a maximum at around 600 nm when excited at 460 nm, as reported previously.[5] In acetonitrile, the complex shows luminescence with a similar intensity to that in water, but the maximum is slightly redshifted. When excited at 460 nm, **3** shows no luminescence in water but exhibits strong emission at around 680 nm in acetonitrile. This behaviour can be attributed to the "light-switch effect" previously reported for **1** and its monomer analogue,[8,31] namely, the quantum yield increases dramatically when the phenazine nitrogen atoms of the dppz moieties are protected from hydrogen bonding by solvent.

Addition of both ct- and AT-DNA to both enantiomers of **2** led to a near doubling of the luminescence intensity, and heating the samples at 50 °C only resulted in small changes in the luminescence intensities. The quantum yield in SDS

micelles was comparable to that in the presence of DNA, preventing studies of the dissociation by fluorescence.

Addition of AT-DNA to **3** in aqueous solution resulted in a slow increase in luminescence with a maximum at approximately 630 nm. This light-switch behaviour indicates that the phenazine nitrogen atoms of the dppz moiety are protected from water when the complex binds to DNA, and one way to achieve this could be by intercalation of the dppz moiety between the base pairs. Interestingly, the ΛΛ enantiomer shows a greater intensity increase than the ΔΔ enantiomer upon addition of AT-DNA, which is in contrast to what was observed for **1**, the ΔΔ enantiomer of which has the higher quantum yield when bound to DNA. Comparison of the final luminescence intensities of both enantiomers of **1** and **3** after 22 h of incubation with AT-DNA at 50 °C shows that both enantiomers of **3** exhibit emission intensities in the same range as ΛΛ-**1**, whereas ΔΔ-**1** shows an intensity approximately 10 times higher (see Figure 5 and Table 1).

Addition of ct-DNA to **3** resulted in an immediate very small increase in luminescence, but virtually no further change in intensity was detected upon incubation of the samples at 50 °C for 22 h.

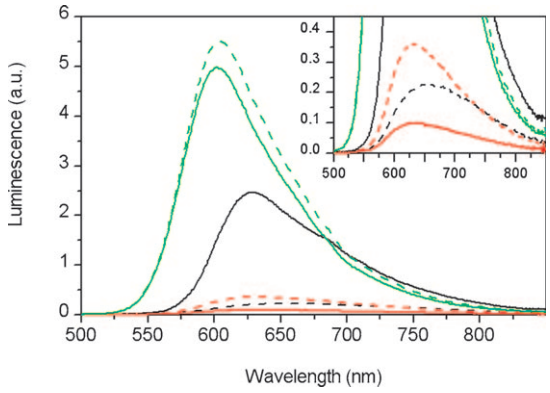

Figure 5. Fluorescence spectra of both enantiomers of complexes **1**–**3** after incubation with AT-DNA in 150 mM NaCl solution for 22 h at 50 °C: ΔΔ-**1** (black solid), ΛΛ-**1** (black dashed), ΔΔ-**2** (green solid), ΛΛ-**2** (green dashed), ΔΔ-**3** (red solid) and ΛΛ-**3** (red dashed). The inset shows an enlargement of the spectra for both enantiomers of **3** and ΛΛ-**1**.

Table 1. Quantum yields, emission lifetimes and pre-exponential factors for complexes **1**–**3** bound to AT-DNA.

Sample[a]	τ_1 [ns] (α_1)	τ_2 [ns] (α_2)	Φ [%][b]	τ_0 [μs][c]
ΔΔ-**1**[d]	62 (0.49)	488 (0.51)	6.4	4.4
ΛΛ-**1**	19 (0.60)	107 (0.40)	0.9	6.0
ΔΔ-**2**	189 (0.27)	1385 (0.73)	15.3	6.9
ΛΛ-**2**	163 (0.26)	1318 (0.74)	18.6	5.5
ΔΔ-**3**	31 (0.80)	520 (0.20)	0.4	32.2
ΛΛ-**3**	33 (0.74)	232 (0.26)	1.5	5.6

[a] 115 μM nucleotides and 3.5 μM complex in 150 mM NaCl at 25 °C. [b] Quantum yields were determined with $[Ru(phen)_2(11,12\text{-dimethyldppz})]^{2+}$ in 1,2-propanediol as a reference. [c] The intrinsic lifetimes were calculated from $\tau_0=(\alpha_1\tau_1+\alpha_2\tau_2)/\Phi$. [d] The values reported here for ΔΔ-**1** deviate slightly from those previously reported in the literature (50 mM NaCl, 8 base pair/complex).[26]

Emission lifetimes and quantum yields: The emission lifetimes measured in the presence of AT-DNA are summarised in Table 1. Two lifetimes were sufficient to fit the data for all samples. The two enantiomers of **2** show similar emission lifetimes, with the longer lifetime being in the microsecond range. This is also reflected by the rather large quantum yields relative to **1** and **3**.

Interestingly, the longer lifetime, which constitutes the major part of the steady-state intensity of **3**, is more than twice as long for ΔΔ-**3** as for ΛΛ-**3**, although the quantum yield is larger for the ΛΛ enantiomer. This indicates that a large fraction of the ΔΔ enantiomer has a lifetime that is too short to be observed in this experiment. The estimated intrinsic lifetimes in the presence of AT-DNA are similar for all complexes except ΔΔ-**3**, probably due to strongly quenched molecules with subnanosecond lifetimes. Assuming that the intrinsic lifetime of ΔΔ-**3** should be in the same range as the others and that 100 % of the molecules of the other complexes have observable lifetimes, the fraction of ΔΔ-**3** with an unobservable lifetime can be calculated to be 80 %, which corresponds to $\tau_0=5.7$ μs.

Kinetics: The kinetics of the interactions between **3** and AT-DNA were investigated by studying the change in luminescence at 625 nm (see Figure 6). Experiments at 25, 37 and

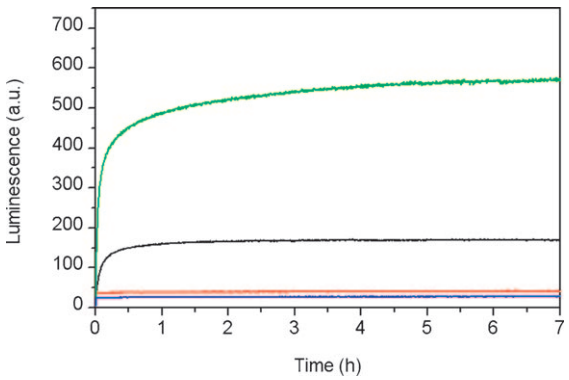

Figure 6. Association kinetics at 50 °C for ΔΔ-**3** in the presence of AT-DNA (black), ΔΔ-**3** in the presence of ct-DNA (red), ΛΛ-**3** in the presence of AT-DNA (green) and ΛΛ-**3** in the presence of ct-DNA (blue).

50 °C revealed slow association kinetics for both enantiomers of the complex and two exponentials were used to fit the initial 7 h of the association process for which the time constants are presented in Table 2. The first rate constant, which is assigned to the primary threading intercalation process,[27] is larger for the ΛΛ enantiomer than for the ΔΔ enantiomer at all temperatures, which indicates faster threading of the ΛΛ enantiomer, although the differences decrease with increasing temperature. Hence, the activation energy, calculated from the Arrhenius equation, is substantially larger for the ΔΔ enantiomer than for the ΛΛ enantiomer (60 and 40 kJ mol^{-1}, respectively). The second rate constant, which is assigned to a redistribution of the threaded complexes, as previously described for complex **1**,[32] similar-

Table 2. Association rate constants and pre-exponential factors for complex **3** in the presence of AT-DNA.[a]

T [°C]	ΔΔ-**3**		ΛΛ-**3**	
	k_1 [10^{-4} s^{-1}] (α_1)	k_2 [10^{-4} s^{-1}] (α_2)	k_1 [10^{-4} s^{-1}] (α_1)	k_2 [10^{-4} s^{-1}] (α_2)
25	4.57 (0.27)	0.38 (0.73)	10.3 (0.57)	0.97 (0.43)
37	13.2 (0.48)	1.52 (0.52)	22.5 (0.61)	1.48 (0.39)
50	34.0 (0.74)	3.64 (0.26)	35.0 (0.65)	1.62 (0.35)

[a] All experiments were performed in 150 mM NaCl solution with 115 μM nucleotides and 3.5 μM complex.

ly shows a stronger temperature dependence for ΔΔ-**3** than for ΛΛ-**3**.

The differences between the final luminescence intensities of the two enantiomers after 22 h of heating at the specified temperatures cannot be explained by the differences in rate constants because after heating for such a long time most of the threading should be completed for both enantiomers, which further supports a smaller fraction of the ΔΔ enantiomer threading AT-DNA in comparison with the ΛΛ enantiomer.

The dissociation kinetics of **3** and AT-DNA were studied at 37 °C by stopped-flow experiments at a concentration of 0.6 % w/w SDS. Two exponentials were required to fit the data for both enantiomers, but the rate constant for the ΛΛ enantiomer ($k_1 = 4.5 \times 10^{-2}\ s^{-1}$ and $k_2 = 1.0 \times 10^{-2}\ s^{-1}$) is nearly half that of the ΔΔ enantiomer ($k_1 = 10 \times 10^{-2}\ s^{-1}$ and $k_2 = 1.9 \times 10^{-2}\ s^{-1}$). Both rate constants for **3** are one to two orders of magnitude larger than the corresponding rate constants for **1**,[8] but still much smaller than those for non-threading intercalators.[11]

Discussion

The increase in luminescence intensity upon addition of both ct- and AT-DNA to **2** has to be regarded as consistent with previously reported results for ct-DNA.[5] Based on viscosity experiments and the fact that the intraligand absorption bands in the UV region showed much greater hypochromicity than the MLCT bands in the visible region upon addition of ct-DNA to the complex, Chao et al. proposed that it is the bridging ligand that interacts with the DNA and that the binding mode is intercalation rather than partial intercalation. However, classic intercalation would, contrary to what was observed in our experiments, be expected to result in good orientation of the DNA in the LD experiments as a result of stiffening and lengthening of the helix upon insertion of the ligand between the base pairs. Instead, the DNA signal in the LD spectra decreased dramatically with increasing concentration of complex, especially for the ΔΔ enantiomer, which indicates decreased orientation of the DNA. For the ΔΔ enantiomer in the presence of ct-DNA, the intensities of both the complex band in the visible region and the DNA band at 260 nm were surprisingly low after heating in comparison with control samples, which indicates condensation of the DNA. This was not observed for the ΛΛ enantiomer, although LD results show that it affects ct-DNA in a similar manner as the ΔΔ enantiomer. However, the ΛΛ enantiomer reduces the orientation of the DNA less efficiently than the ΔΔ enantiomer, which means that it is possible that complete condensation of the DNA would also occur with the ΛΛ enantiomer, but at higher concentrations of the complex.

The ability of ΔΔ-**2** to condense DNA is quite impressive (1:10 complex/base-pair ratio for complete condensation) compared with other cationic DNA condensing agents such as polyamines (spermine and spermidine), cobalt and binuclear iron complexes. The DNA condensation properties of these molecules have been studied by LD by Rodger et al.[33] and it was found that approximately molecule/base-pair ratio of 1:1.5 was required for complete disappearance of the LD signal for the most efficient of the examined substances.[33]

Note also that even though the pure enantiomers of **2** do not seem to intercalate ct-DNA, intercalation cannot be ruled out as a binding mode for the racemic mixture. It is possible that the *meso* stereoisomer, which is likely to form 50 % of the racemic mixture, binds ct-DNA in a different way to the ΔΔ and ΛΛ enantiomers.

In vivid contrast to the absence of LD signals for complex **2**, both enantiomers of the hybrid complex **3** show strong and very similar LD bands with ct-DNA. The reduced LD of the phenanthroline $\pi \rightarrow \pi^*$ transition dipole moment below 300 nm is very sensitive to rotation of the phenanthroline ligands around the bridging ligand axis, which might give rise to large differences between the enantiomers.[26] Because the values of the reduced LD are nearly identical for the two enantiomers in this region, it is likely that the bridging ligand is in its planar conformation and that the complex as a whole does not roll in the DNA-bound state. The angle between the long-axis polarised transitions of the complex and the DNA helix axis was calculated to be around 70°, which indicates partial intercalation rather than classic groove binding that most likely occurs from the major groove in view of the size of the complex.

Because **2** shows a similar luminescence intensity in the presence and absence of DNA as well as in the presence of SDS, the association and dissociation kinetics could not be studied with accuracy by fluorescence spectroscopy. Neither was LD an option because no complex signal could be detected because of the loss of orientation of the ct-DNA in the presence of the complex and the AT-DNA being too short to obtain sufficient orientation of the samples. However, it is unlikely that the binding mode is threading intercalation in the presence of ct-DNA because this would result in an increased rather than decreased orientation of the sample as a result of stiffening and lengthening of the DNA molecules. Neither is threading intercalation likely to occur in the presence of AT-DNA because the changes in absorbance and luminescence are similar to those observed in the presence of ct-DNA. This is in contrast to what we expected; we envisaged that a more flexible bridge would be bene-

ficial for threading intercalation because the threading of **1** has been suggested to induce large conformational changes in AT-DNA.[34] A more flexible bridge has the ability to adapt its structure to fit the DNA better and hence subject the DNA to less stress upon binding. However, the conformational freedom of **2** seems rather to favour accommodation in one of the grooves. Hydrogen bonding of the imidazole hydrogen to one of the bases or the DNA backbone when situated in the groove or a decrease in the hydrophobic interactions in the threaded state due to the smaller hydrophobic surface of the bridging ligand may also contribute to the shift of the equilibrium towards groove binding.

However, it was surprising to find that **3**, with a shorter and more rigid bridge, binds AT-DNA by threading intercalation. The rate constant for the SDS-induced dissociation of **3** bound to AT-DNA is very small in comparison with common intercalators such as daunomycin[11] and non-threaded, groove-bound **1**, which supports threading intercalation as the binding mode even though it is still approximately one order of magnitude larger than the dissociation rate constant of **1** when threaded through ct-DNA.[8] This, in addition to the lower association rates of **3**, means that **3** is a weaker threading intercalator than **1**.

The lower association rates of **3** could be explained by stronger interactions in the groove-bound state, higher activation energy for the threading process, less favourable interactions with the DNA in the threaded state or a combination of these explanations. Comparison of the activation energies for **3** (~60 and ~40 kJ mol^{-1} for the ΔΔ and ΛΛ enantiomers, respectively) and **1** (97 kJ mol^{-1} for the ΛΛ enantiomer[12]) shows that the low threading rate cannot be explained in terms of activation energies. For the ΔΔ enantiomer, which, in contrast to what has been observed for **1**, is a poorer threading intercalator than the ΛΛ enantiomer,[12] the low threading rate can be explained by the fact that only 20% of the complex is threaded at equilibrium, as judged by emission lifetime experiments. This would result in an equilibrium constant of less than 1, which in turn means that the dissociation rate constant is larger than the association rate constant and that the observed rate constant in the association studies is in fact the dissociation rate constant.

However, this explanation does not hold for the ΛΛ enantiomer, which appears to have an equilibrium constant larger than 1. Instead, we suggest an explanation based on the binding model proposed by Nordell et al.[34] in which the complex initially binds in the groove of B-form DNA and initiates a conformational change of the DNA to an intermediate state with a more A-form-like structure. The actual threading of the complex then occurs in the A-form conformation through base-pair opening. The formation of A-DNA does not require breakage of any bonds, which makes it more conceivable that the concomitant increase in free energy is mainly due to a decrease in entropy, whereas the base-pair opening involves breakage of hydrogen bonds, which is likely to give rise to an appreciable activation energy. If the entropy decrease accompanying the conformational change from B- to A-form DNA is larger for **3** than for **1** and more energy is required to open up the base pair in the case of complex **1**, it is possible that the threading of complex **3** has a higher free energy of activation than **1**. This would explain the lower association rates of **3** despite the lower activation energy.

As noted above, there is no indication of the threading intercalation of **3** in the presence of ct-DNA. This enormous selectivity for threading in AT-DNA is surprising because even though threading intercalation of **1** is kinetically selective for long AT stretches, it still threads mixed-sequence DNA to some extent given sufficient time at elevated temperatures. Clearly the shorter and more rigid bridge makes threading intercalation even more sensitive to the flexibility of the DNA. A plausible explanation for this is that the stress on the DNA increases with the shorter bridge because the distance between the bulky ruthenium centres decreases, which may lead to severe distortions of the DNA helix structure due to steric interactions between the phenanthroline ligands and the DNA in the threaded state. By shortening the bridge, we seem to have shifted the equilibrium between partial groove intercalation and threading intercalation towards the former, and because the free energy of complex **1** threaded in ct-DNA is higher than when threaded in AT-DNA, threading of complex **3** in ct-DNA has a higher free energy than the initial partial groove intercalated state assuming a similar energy difference between ct- and AT-DNA as for **1**. Thus, threading of complex **3** in ct-DNA is thermodynamically unfavourable whereas threading in AT-DNA still occurs although with an equilibrium constant smaller than that for the ΔΔ enantiomer.

Steric interactions between the DNA and the phenanthroline ligands in the threaded state may also be the reason for the reversed enantioselectivity. For **1**, steric interactions with the phenanthroline ligands connected to the non-intercalating half of the complex are not likely to exert any severe stress on the DNA, but if these ligands are moved closer to the DNA helix they may cause distortions of the DNA structure. Hence the geometry around this ruthenium centre may come to dominate the enantioselectivity for the complex with the shorter bridge whereas the geometry around the ruthenium centre of the intercalated part may be more important when the bridge is longer. However, the emission lifetime of ΔΔ-**3** when threaded in AT-DNA is considerably longer than for the ΛΛ enantiomer, which indicates that the dppz ligand of the ΔΔ enantiomer is better protected from water in the threaded state. This suggests that the dppz ligand of the threaded ΔΔ enantiomer is inserted deeper into the base-pair stack than the dppz ligand of the ΛΛ enantiomer despite the fact that ΔΔ-**3** has a smaller equilibrium constant than the ΛΛ enantiomer.

Conclusion

The effect of bridging ligand structure on threading intercalation ability has been investigated and it was found that a

shorter bridge seems to impair threading intercalation in terms of both association and dissociation rates as well as degree of binding. A shorter bridge also makes the threading process more sensitive to DNA flexibility. However, conserving the length of the bridging ligand is not sufficient for retaining threading efficiency; the dppz moiety also seems crucial for threading intercalation to occur. This is probably because the extended ring system of the dppz moiety enables more favourable interactions with DNA bases in the threaded state than the smaller ring system of the imidazophenanthroline moiety. Also, it is possible that some degree of rigidity in the bridging ligand is necessary to distort the DNA structure enough to initiate the threading process. In conclusion, it has been shown that the length and rigidity of the bridging ligand as well as the size of the intercalated ring system are all factors that strongly influence the efficiency of threading intercalation. Finally, it should also be noted that changing the bridging ligand changes the enantioselectivity.

Experimental Section

Sample preparation: All experiments were conducted in 150 mM NaCl solution (1 mM cacodylate, pH 7.0). The highly polymerised type I sodium salt of calf thymus DNA, purchased from Sigma, was dissolved in 150 mM NaCl solution and filtered through a 0.8 μm Millipore filter before use. Polydeoxyadenylic-thymidylic acid sodium salt (poly(dAdT)$_2$), purchased from Sigma, was dissolved in 150 mM NaCl solution and used without further purification. The concentrations of DNA were estimated by using $\varepsilon_{260nm}=6600\ M^{-1}cm^{-1}$ for calf thymus DNA and $\varepsilon_{262nm}=6600\ M^{-1}cm^{-1}$ for poly(dAdT)$_2$. For [μ-bidppz(phen)$_4$Ru$_2$]$^{4+}$, $\varepsilon_{262nm}=200\,000\ M^{-1}cm^{-1}$ was calculated from the previously reported value of $\varepsilon_{408nm}=75\,800\ M^{-1}cm^{-1}$[32] and used for the other two complexes because changing the bridging ligand did not significantly affect the shape of the absorption band of the phenanthroline ligands at around 260 nm. The concentrations used in the experiments were approximately 115 μM nucleobases and 3.5 μM ruthenium complex giving a ratio of [base pair]/[complex] of around 16. For dissociation experiments a stock solution of 3% w/w SDS in 150 mM NaCl solution was mixed with preincubated samples of DNA and ruthenium complex to a final concentration of 0.6% (stopped-flow) or 0.5% (linear dichroism) detergent.

Instrumentation: Absorption measurements were performed on Varian Cary 4000 UV-Vis and Cary 4 Bio UV-Vis spectrophotometers with a 150 mM NaCl solution as baseline.

Fluorescence measurements were performed on a Varian Cary Eclipse spectrofluorimeter. Emission spectra were recorded at an excitation wavelength of 460 nm and normalised against the corresponding emission spectra recorded at 355 nm excitation at which all samples had equal absorbance. In the association kinetics experiments, the samples were excited at 460 nm and emission was recorded at 625 nm.

Dissociation kinetics were studied at 37°C with a Chirascan CD spectropolarimeter equipped with a stopped-flow device and a fluorescence detector. The samples were excited at 355 nm and the total emission intensity above 395 nm was collected at an angle perpendicular to the excitation light. The emission intensity was studied for 200 s for ΔΔ-**3** and 300 s for ΛΛ-**3**, and 10 kinetic traces, obtained with the pressure hold-function activated, were averaged for each sample.

Linear dichroism (LD) was measured by using a Jasco J-720 CD spectropolarimeter, equipped with an Oxley prism to obtain linearly polarised light, on samples oriented in an outer-rotating Couette flow cell with a 1 mm path length.[35,36] Spectra were measured at a shear gradient of 3000 s^{-1} and corrected for baseline contributions by subtraction of the corresponding spectra recorded without rotation.

Circular dichroism (CD) was performed on a Jasco J-810 spectropolarimeter with a 150 mM NaCl solution as baseline.

Nanosecond emission decays were measured by using the third harmonic of a Nd:YAG laser (Continuum Surelite II-10, pulse width <7 ns) to provide an excitation wavelength of 355 nm. The emitted light was detected with a Hamamatsu R928 photomultiplier tube at an angle of 90° relative to the excitation light. The monitoring wavelength was set to 630 nm. The decays were collected and averaged with a 200 MHz digital oscilloscope (Tetronix TDS2200 2Gs/s) and stored in a Lab View program (developed at the department), which also controls the instrument set-up. The kinetic traces were obtained by averaging 48 recorded decay curves.

Data analysis: Quantum yields were obtained by comparison of the integrated corrected emission spectra with that of [Ru(phen)$_2$-11,12-dimethyldppz]$^{2+}$ in 1,2-propanediol purged with nitrogen ($\Phi=7.7\%$).[37] Integration was carried out on the energy scale using the *trapz* function in the Matlab software package (Mathworks, Inc.; www.mathworks.com).

Kinetic traces (DNA association/dissociation and luminescence decays) were projected onto the space spanned by one, two or three exponentials using the matrix pseudoinverse function *pinv* in the Matlab software package (Mathworks, Inc.). The (Euclidian) norm of the residual was minimised by varying the rate constant with the simplex algorithm using the Matlab function *fminsearch*. A fit was judged acceptable if the residual was unstructured and inclusion of a further exponential did not decrease the residual norm by more than 30%. According to these criteria, two exponentials were needed to fit the emission decay data for all samples and the kinetic data for all samples except ΛΛ-dppzip at 50°C, for which three exponentials gave a slightly larger residual norm decrease of 45%.

Linear dichroism[35] is defined as the difference in absorbance of linearly polarised light, parallel and perpendicular to a macroscopic orientation axis [here the flow direction; Eq. (1)].

$$LD = A_{||} - A_{\perp}$$

The LD spectrum is a weighted sum of the differently polarised absorption envelopes $\varepsilon_i(\lambda)$ such that the isotropic absorption spectrum is given by Equation (2) and the linear dichroism spectrum by Equation (3) in which S is the global orientation factor ($0 \le S \le 1$), which here measures how well the helix axis of DNA is aligned in the flow field. The weights w_i depend on the angle α_i between the transition moment i and the helix axis [Eq. (4)].

$$A_{iso}(\lambda) = \Sigma\varepsilon_i(\lambda)$$

$$LD(\lambda) = S\Sigma w_i\varepsilon_i(\lambda)$$

$$w_i = 1.5(3\cos^2\alpha_i - 1)$$

The reduced linear dichroism LD^r is the LD divided by the isotropic absorption [Eq. (5).

$$LD^r(\lambda) = LD^r(\lambda)/A_{iso}(\lambda) = S\Sigma w_i\varepsilon_i(\lambda)/\Sigma\varepsilon_i(\lambda)$$

In those regions of the spectrum in which the transition moments have the same polarisation direction, the reduced linear dichroism is independent of the wavelength [Eq. (6)].

$$LD^r = S\Sigma w_i\varepsilon_i(\lambda)/\Sigma\varepsilon_i(\lambda) = Sw_i\Sigma\varepsilon_i(\lambda)/\Sigma\varepsilon_i(\lambda) = Sw_i$$

An estimate of the orientation factor S can be obtained from the LD^r in the nucleobase absorption region at around 260 nm, at which w_i is −1.5 for an ideal B-DNA conformation in which the nucleobase planes are oriented perpendicular to the helix axis ($\alpha=90°$ for $\pi\rightarrow\pi^*$ transitions).

General information for the syntheses: Ammonium acetate (Merck), tetra-*n*-butylammonium chloride (Fluka), pyridinium chlorochromate, ammonium hexafluorophosphate and isophthalaldehyde (Sigma–Aldrich)

were used as received without further purification. Analytical thin-layer chromatography was performed on Merck silica gel, grade 60 F_{254}, with acetonitrile/ethanol/$NaNO_3$(aq. 10% w/w) (1:1:1) as eluent. ^{1}H NMR spectra were recorded on a Varian UNITY-VXR 5000 (400 MHz) spectrometer and chemical shifts are reported with [D_6]DMSO (δ_H = 2.50 ppm) as reference. Mass spectra were recorded on a Bruker Autoflex MALDI-TOF instrument using 2,5-dihydroxybenzoic acid as the matrix. Elemental analysis of compound **3** was performed on the PF_6 salt at the Mikroanalytisches Laboratorium Kolbe in Mülheim (Germany).

Synthesis of Δ- and Λ-bis(1,10-phenanthroline)(1,10-phenanthroline-5,6-dione)ruthenium bis(hexafluorophosphate) (a): Compound **a** was synthesised and resolved into the pure enantiomers following the method previously reported by Hiort et al.[29]

Synthesis of ΔΔ-[μ-bipb(phen)$_4$Ru$_2$]Cl$_4$ (2): Enantiomer Δ-**a** (114 mg, 0.12 mmol), isophthalaldehyde (**b**; 7 mg, 0.054 mmol) and ammonium acetate 185 mg, 2.4 mmol) were dissolved in acetonitrile/acetic acid (1:1, 1.7 mL). The solution was heated in a screw-capped vial in a boiling water bath for 2 h and then cooled to room temperature. The product was precipitated with aqueous ammonium hexafluorophosphate, filtered, washed with water and diethyl ether and then purified by column chromatography on alumina oxide (neutral, activity grade super I) with acetonitrile/ethanol (3:1) as eluent. After evaporation of the solvent the product was dissolved in a small volume of acetonitrile and the chloride salt was precipitated by the addition of tetra-*n*-butylammonium chloride in acetone. The resulting orange-red solid was filtered off and washed with acetone. R_f~0.3; ^{1}H NMR (400 MHz, [D_6]DMSO): δ = 9.60 (s, 1H), 9.54 (br s, 2H), 9.15 (br s, 2H), 8.79 (d, J = 8.0 Hz, 8H), 8.69 (d, J = 8.0 Hz, 2H), 8.40 (s, 8H), 8.16 (d, J = 4.8 Hz, 4H), 8.09 (d, J = 5.2 Hz, 4H), 8.04 (d, J = 4.4 Hz, 4H), 7.92 (t, J = 7.2 Hz, 1H), 7.84 (br m, 4H), 7.78 ppm (m, 8H). MS (MALDI-TOF): m/z: calcd for $[M]^+$: 1438.2; found: 1436.9 $[M-H]^+$; CD (150 mM aq. NaCl): λ_{extr} ($\Delta\varepsilon$) = 258 (306), 270 (−384), 300 (−301), 426 (38), 472 nm (−34 dm^{3}mol^{-1}cm^{-1}).

Synthesis of Δ- and Λ-bis(1,10-phenanthroline)(11-hydroxymethyldipyrido[3,2-*a*:2′-3′-*c*]phenazine)ruthenium bis(hexafluorophosphate) (e): The synthesis of the pure enantiomers of **e** is described elsewhere.[30]

Synthesis of Δ-bis(1,10-phenanthroline)(dipyrido[3,2-*a*:2′,3′-*c*]phenazine-11-carboxaldehyde)ruthenium bis(hexafluorophosphate) (f): A mixture of Δ-**e** (11 mg, 0.01 mmol) and pyridinium chlorochromate (4 mg, 0.02 mmol) in acetonitrile (0.5 mL) was stirred at 50 °C until the over-oxidised carboxylic acid (R_f~0.2) appeared on the TLC plates. The solvent was evaporated under reduced pressure. The solid residue was washed with water (3 × 10 mL) to remove excess pyridinium chlorochromate and dried in vacuum to give a red-orange powder (9 mg, 80%). R_f~0.6; ^{1}H NMR (400 MHz, [D_6]DMSO): δ = 7.76–7.84 (m, 4H), 7.91–7.95 (m, 2H), 8.06 (d, J = 5.2 Hz, 2H), 8.22 (d, J = 4.8 Hz, 2H), 8.27 (d, J = 4.8 Hz, 2H), 8.41 (s, 4H), 8.50 (d, J = 9.6 Hz, 1H), 8.65 (d, J = 9.6 Hz, 1H), 8.80 (t, J = 8.0 Hz, 4H), 9.14 (s, 1H), 9.63 (d, J = 8.0 Hz, 2H), 10.45 ppm (s, 1H).

Synthesis of ΔΔ-[μ-dppzip(phen)$_4$Ru$_2$]Cl$_4$ (3): Complex **3** was prepared by treating Δ-**a** with an equimolar amount of Δ-**f** in the presence of ammonium acetate following the same procedure as described above for **2**. The formation of a binuclear complex (R_f~0.3) was confirmed by TLC along with complex **1** (R_f~0.2) and **2** (R_f~0.3) as well as mononuclear ruthenium complexes (R_f values between 0.5 and 0.6) as reference compounds. Acetonitrile was used as eluent in the column chromatography. ^{1}H NMR (400 MHz, [D_6]DMSO): δ = 9.88 (br s, 1H), 9.80 (s, 1H), 9.64 (d, J = 8.2 Hz, 2H), 9.34 (d, J = 8.7 Hz, 1H), 9.17 (d, J = 8.2 Hz, 1H), 8.81 (m, 8H), 8.73 (d, J = 8.7 Hz, 1H), 8.42 (d, J = 3.2 Hz, 8H), 8.31 (d, J = 5.5 Hz, 2H), 8.23 (t, J = 6.9 Hz, 2H), 8.18 (d, J = 5.5 Hz, 2H), 8.08 (m, 6H), 7.96 (m, 3H), 7.90–7.76 ppm (m, 10H); MS (MALDI-TOF): m/z: calcd for $[M]^+$: 1424.2; found: 1422.9 $[M-H]^+$; elemental analysis calcd (%) for $C_{79}H_{48}F_{24}N_{16}P_4Ru_2$·3.5$H_2O$: C 45.92, H 2.68, N 10.85; found: C 45.88, H 2.52, N 10.68; CD (150 mM aq. NaCl): λ_{extr} ($\Delta\varepsilon$) = 256 (286), 268 (−548), 299 (−214), 425 (33), 470 nm (−43 dm^{3}mol^{-1}cm^{-1}).

The corresponding enantiomers ΛΛ-**2** and ΛΛ-**3** were synthesised analogously from Λ-**a** and Λ-**f**. The analytical data (NMR, MS, UV-Vis) were identical to those of the corresponding Δ enantiomer. The CD spectra of the Λ enantiomers of complexes **2** and **3** were mirror images of those of the corresponding Δ enantiomer (see Figure 3) within 2% error.

Acknowledgements

This work was funded by The Swedish Research Council (VR). The authors gratefully acknowledge Renée Kroon for help with the MALDI-TOF mass spectrometry and Anna Reymer for drawing Figure 1.

[1] J. K. Barton, A. T. Danishefsky, J. M. Goldberg, *J. Am. Chem. Soc.* **1984**, *106*, 2172–2176.
[2] C. Metcalfe, J. A. Thomas, *Chem. Soc. Rev.* **2003**, *32*, 215–224.
[3] C. Moucheron, *New J. Chem.* **2009**, *33*, 235–245.
[4] J. A. Smith, J. L. Morgan, A. G. Turley, J. G. Collins, F. R. Keene, *Dalton Trans.* **2006**, 3179–3187.
[5] H. Chao, Y. X. Yuan, F. Zhou, L. N. Ji, J. Zhang, *Transition Met. Chem.* **2006**, *31*, 465–469.
[6] F. R. Liu, K. Z. Wang, G. Y. Bai, Y. G. Zhang, L. H. Gao, *Inorg. Chem.* **2004**, *43*, 1799–1806.
[7] F. O'Reilly, J. Kelly, A. Kirsch-De Mesmaeker, *Chem. Commun.* **1996**, 1013–1014.
[8] L. M. Wilhelmsson, F. Westerlund, P. Lincoln, B. Norden, *J. Am. Chem. Soc.* **2002**, *124*, 12092–12093.
[9] W. Muller, D. M. Crothers, *J. Mol. Biol.* **1968**, *35*, 251–290.
[10] C. K. Smith, G. J. Davies, E. J. Dodson, M. H. Moore, *Biochemistry* **1995**, *34*, 415–425.
[11] K. R. Fox, C. Brassett, M. J. Waring, *Biochim. Biophys. Acta Gen. Subj.* **1985**, *840*, 383–392.
[12] P. Nordell, F. Westerlund, L. M. Wilhelmsson, B. Norden, P. Lincoln, *Angew. Chem.* **2007**, *119*, 2253–2256; *Angew. Chem. Int. Ed.* **2007**, *46*, 2203–2206.
[13] Z. S. Juo, T. K. Chiu, P. M. Leiberman, I. Baikalov, A. J. Berk, R. E. Dickerson, *J. Mol. Biol.* **1996**, *261*, 239–254.
[14] N. A. Davis, S. S. Majee, J. D. Kahn, *J. Mol. Biol.* **1999**, *291*, 249–265.
[15] M. J. Gardner, N. Hall, E. Fung, O. White, M. Berriman, R. W. Hyman, J. M. Carlton, A. Pain, K. E. Nelson, S. Bowman, I. T. Paulsen, K. James, J. A. Eisen, K. Rutherford, S. L. Salzberg, A. Craig, S. Kyes, M. S. Chan, V. Nene, S. J. Shallom, B. Suh, J. Peterson, S. Angiuoli, M. Pertea, J. Allen, J. Selengut, D. Haft, M. W. Mather, A. B. Vaidya, D. M. A. Martin, A. H. Fairlamb, M. J. Fraunholz, D. S. Roos, S. A. Ralph, G. I. McFadden, L. M. Cummings, G. M. Subramanian, C. Mungall, J. C. Venter, D. J. Carucci, S. L. Hoffman, C. Newbold, R. W. Davis, C. M. Fraser, B. Barrell, *Nature* **2002**, *419*, 498–511.
[16] J. L. Morgan, D. P. Buck, A. G. Turley, J. G. Collins, F. R. Keene, *Inorg. Chim. Acta* **2006**, *359*, 888–898.
[17] F. M. Foley, F. R. Keene, J. G. Collins, *J. Chem. Soc. Dalton Trans.* **2001**, 2968–2974.
[18] C. W. Jiang, *Eur. J. Inorg. Chem.* **2004**, 2277–2282.
[19] C. W. Jiang, *Inorg. Chim. Acta* **2005**, *358*, 1231–1236.
[20] C. W. Jiang, H. Chao, X. L. Hong, H. Li, W. J. Mei, L. N. Ji, *Inorg. Chem. Commun.* **2003**, *6*, 773–775.
[21] J. L. Morgan, D. P. Buck, A. G. Turley, J. G. Collins, F. R. Keene, *J. Biol. Inorg. Chem.* **2006**, *11*, 824–834.
[22] X. H. Zou, B. H. Ye, H. Li, J. G. Lin, Y. Xiong, L. N. Ji, *J. Chem. Soc. Dalton Trans.* **1999**, 1423–1428.
[23] L. Mishra, A. K. Yadaw, S. Srivastava, A. B. Patel, *New J. Chem.* **2000**, *24*, 505–510.
[24] F. M. O'Reilly, J. M. Kelly, *New J. Chem.* **1998**, *22*, 215–217.
[25] J. Z. Wu, L. Yuan, *J. Inorg. Biochem.* **2004**, *98*, 41–45.
[26] F. Westerlund, M. P. Eng, M. U. Winters, P. Lincoln, *J. Phys. Chem. B* **2007**, *111*, 310–317.
[27] F. Westerlund, P. Nordell, J. Blechinger, T. M. Santos, B. Norden, P. Lincoln, *J. Phys. Chem. B* **2008**, *112*, 6688–6694.

[28] B. Önfelt, P. Lincoln, B. Norden, *J. Am. Chem. Soc.* **2001**, *123*, 3630–3637.
[29] C. Hiort, P. Lincoln, B. Norden, *J. Am. Chem. Soc.* **1993**, *115*, 3448–3454.
[30] M. Li, P. Lincoln, *J. Inorg. Biochem.* **2009**, *103*, 963–970.
[31] A. E. Friedman, J. C. Chambron, J. P. Sauvage, N. J. Turro, J. K. Barton, *J. Am. Chem. Soc.* **1990**, *112*, 4960–4962A.
[32] F. Westerlund, L. M. Wilhelmsson, B. Norden, P. Lincoln, *J. Phys. Chem. B* **2005**, *109*, 21140–21144.
[33] A. Rodger, K. J. Sanders, M. J. Hannon, I. Meistermann, A. Parkinson, D. S. Vidler, I. S. Haworth, *7th International Conference on Circular Dichroism (CD 99)* (Mierki, Poland), **1999**, pp. 221–236.
[34] P. Nordell, F. Westerlund, A. Reymer, A. H. El-Sagheer, T. Brown, B. Nordén, P. Lincoln, *J. Am. Chem. Soc.* **2008**, *130*, 14651–14658.
[35] B. Norden, M. Kubista, T. Kurucsev, *Q. Rev. Biophys.* **1992**, *25*, 51–170.
[36] B. Norden, S. Seth, *Appl. Spectrosc.* **1985**, *39*, 647–655.
[37] J. Olofsson, L. M. Wilhelmsson, P. Lincoln, *J. Am. Chem. Soc.* **2004**, *126*, 15458–15465.

Received: January 22, 2010
Revised: June 1, 2010
Published online: August 2, 2010

